J Therm Anal Calorim (2012) 107:407–412
DOI 10.1007/s10973-011-1841-x

# Thermal decomposition kinetics of magnesite from thermogravimetric data

**X. W. Liu · Y. L. Feng · H. R. Li · P. Zhang · P. Wang**

Received: 8 July 2010 / Accepted: 2 August 2011 / Published online: 19 August 2011


**Abstract** Thermal decomposition kinetics of magnesite were investigated using non-isothermal TG-DSC technique at heating rate ($\beta$) of 15, 20, 25, 35, and 40 K min$^{-1}$. The method combined Friedman equation and Kissinger equation was applied to calculate the $E$ and lg$A$ values. A new multiple rate iso-temperature method was used to determine the magnesite thermal decomposition mechanism function, based on the assumption of a series of mechanism functions. The mechanism corresponding to this value of $F(a)$, which with high correlation coefficient ($r$-squared value) of linear regression analysis and the slope was equal to $-1.000$, was selected. And the Malek method was also used to further study the magnesite decomposition kinetics. The research results showed that the decomposition of magnesite was controlled by three-dimension diffusion; mechanism function was the anti-Jander equation, the apparent activation energy ($E$), and the pre-exponential term ($A$) were 156.12 kJ mol$^{-1}$ and $10^{5.61}$ s$^{-1}$, respectively. The kinetic equation was

$$\frac{d\alpha}{dT} = \frac{10^{5.61}}{\beta}\exp\left(-\frac{18777.9}{T}\right) \times \left\{\frac{3}{2}(1+\alpha)^{2/3}[(1+\alpha)^{1/3}-1]^{-1}\right\},$$

and the calculated results were in accordance with the experiment.

X. W. Liu · Y. L. Feng (✉) · P. Zhang · P. Wang
Civil and Environmental Engineering School, University of Science and Technology, Beijing 100083, China
e-mail: ylfeng126@126.com

H. R. Li
National Key State Laboratory of Biochemical Engineering, Institute of Process Engineering, Chinese Academy of Science, Beijing 100190, China

**Keywords** Magnesite · TG-DSC · Thermal decomposition · Reaction mechanism · Linear regression

**List of symbols**

| | |
|---|---|
| $E$ | Activation energy, kJ mol$^{-1}$ |
| $A$ | Pre-exponential factor, s$^{-1}$ |
| $\alpha$ | Conversion factor |
| $\beta$ | Heating rate, K min$^{-1}$ |
| $R$ | Universal gas constant, 8.314 kJ mol$^{-1}$ K$^{-1}$ |
| $T$ | Temperature, K |
| $r$ | Regression coefficient |
| $T_{max}$ | Temperature at the maximum reaction rate, K |

## Introduction

With the reserves, production, and export volume ranking the first in the world, Magnesite ($MgCO_3$) is a mineral resources advantage in China [1]. It is a main raw material in magnesium industry and refractory industry [2, 3], and widely used in building materials, chemical, paper, aerospace, automobile, and environmental protection [4]. Industrial magnesia and activity magnesium oxide are typically produced from magnesite by calcining directly. Research on thermal decomposition kinetics of magnesite enable us to better understand the decomposition mechanism, control steps, and the various factors on the process of thermal decomposition, thereby allowing us to optimize the thermal decomposition conditions for the high efficient use of magnesite. However, thermal decomposition kinetics of magnesite is rarely researched, so research on the thermal decomposition mechanism of magnesite is of great significance.

The aim of the study was to investigate the thermal decomposition of magnesite by TG-DTG technology [5, 6]. Based on the analysis of the thermal decomposition

dynamic parameters, the magnesite decomposition mechanism was investigated and the key dynamic parameters were also tested.

## Experimental

### Materials

Raw materials used in this study are listed as follows: Natural magnesite was supplied by Haicheng in Liaoning Province. From chemical analysis the natural magnesite contained 46.7% MgO, 1.35% CaO, 0.52% $SiO_2$, 0.41% $Fe_2O_3$, 0.05% $Al_2O_3$, and 50.97% Ignition loss.

### *TG analysis*

The ore was crushed and sieved to 0.45 mm for TG and DSC data. The calcination experiments were carried in the temperature range between 25 and 900 °C. Decomposition works were carried out using a NETZSCH STA 449C thermal analysis instrument TG-DSC system. For TG and DSC, a given amount of sample was put into an Alumina crucible and its mass loss was recorded at heating rate of 15, 20, 25, 35, and 40 K $min^{-1}$ in an $N_2$ gas flow. In the TG-DSC system, masses of sample of 18.915 mg were used, and the results obtained were repeatable.

## Results and discussion

### Decomposition of magnesite

TG and DSC curves of the ore are given in Fig. 1.

The TG-DSC curves indicate that magnesite decomposited completely when the temperature was in the range of 400–800 °C, which is slightly different from the literature [7]. This is mainly due to operational conditions, the structure, and composition of different mineral. In the temperature program process, different heating rates have the same trend of TG-DSC. DSC downward peaks correspond with weight loss steps of the TG curves, and its weight loss rate are basically the same. As the thermal decomposition of magnesite need to absorb heat, it results in the appearance of DSC curves with downward peaks. TG curve is only one weight loss step corresponding to an endothermic peak, and it shows that the thermal decomposition of magnesite belong to one-step reaction [8].

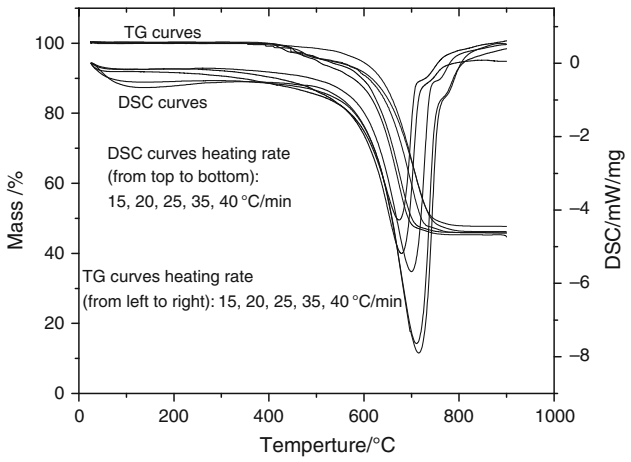


**Fig. 1** TG and DSC diagram of magnesite ore

### *Dynamic parameters calculation*

According to non-isothermal kinetic theory, the kinetic equation of solid-state thermal transformation under linear temperature increasing condition could be generally described as [9–12]:

$$\frac{d\alpha}{dt} \equiv \beta \frac{d\alpha}{dt} = k(T)f(\alpha) = A\exp\left(\frac{-E}{RT}\right)f(\alpha) \quad (1)$$

where $\alpha$ represents the extent of reaction, which can be determined from TG curves as a fractional mass loss, $\beta$ is the linear heating rate, $t$ is time, $k(T)$ a temperature dependent rate constant usually expressed by an Arrhenius-type expression with $A$, and $E$ the pre-exponential factor and the activation energy, respectively and $f(\alpha)$ denotes the particular reaction model, which describes the dependence of the reaction rate on the extent of reaction.

In Eq. 1, the mutual dependence of the Arrhenius parameters $A$ and $E$, which are affected by the choice of the kinetic model function, $f(\alpha)$, recommends that at least one of the kinetic triplet [$A$, $E$, $f(\alpha)$] elements should be computed independently from the others. In this study, to estimate the kinetic parameters of magnetized thermal decomposition both Friedman equation and Kissinger equation were used.

Simple rearrangement of Eq. 1 leads to Eq. 2, which forms the foundation of the differential isoconversional method of Friedman [13, 14]:

$$\ln\left(\frac{d\alpha}{dt}\right)_{\alpha,i} \equiv \ln\left(\beta_i \frac{d\alpha}{dt}\right)_{\alpha} = \ln[A_\alpha f(\alpha)] - \frac{E}{RT_{\alpha,i}} \quad (2)$$

where the subscript $\alpha$ denotes value at a specific of reaction and the subscript $i$ denotes different heating rates. From Eq. 2 we can see that: under $\beta$ diversity and $\alpha$ value are identical situation, by plotting $\ln \beta(d\alpha/dT) - (1/T)$-curves, a straight line can be produced, from which slopes can be used to calculate $E$, which obtained without the involvement of mechanism functions [15].

In this study, the experiments were conducted at five heating rates of 15, 20, 25, 35, and 40 K $min^{-1}$. The curve, when $\alpha = 20\%$, was shown in Fig. 2.

Under different conversions, the magnesite decomposition activation energy was calculated by the same method.

Kissinger equation [16] can be written as:

$$\ln\frac{\beta}{T_m^2} = \ln\frac{AR}{E} - \frac{E}{RT_m} \tag{3}$$

According to Kissinger method $E$ and $A$ can be determined from a plot of the logarithm of the heating rate over the squared temperature at the maximum reaction rate, $T_{max}$, versus the inverse of $T_{max}$ in constant heating rate experiments. Where $T_{max}$ is the temperature corresponding to the inflection point of the thermo-degradation curve, which corresponds to the maximum reaction rate. The $\ln(\beta/T_m^2) \sim 1/T_m$ curve was shown in Fig. 3.

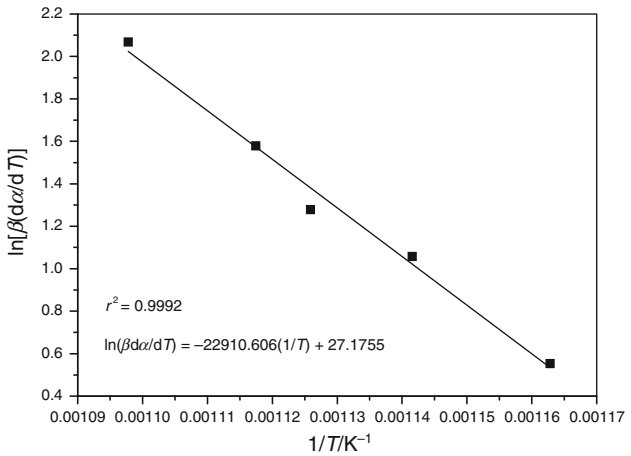


**Fig. 2** The $\ln(\beta(d\alpha/dT)) - (1/T)$ curve when conversion $\alpha = 0.20$

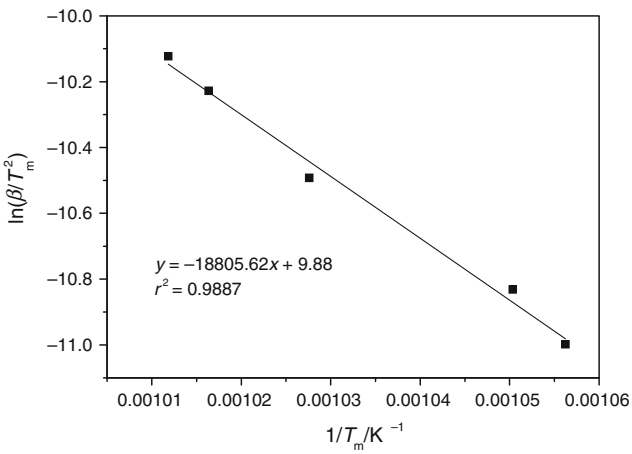


**Fig. 3** The $\ln(\beta/T_m^2) \sim 1/T_m$ curve

**Table 1** Kinetic parameters of magnesite thermal decomposition.

| Method | $E$/kJ $mol^{-1}$ | lg$A$/$s^{-1}$ | $r^2$ |
|---|---|---|---|
| Friedman equation | 155.89 | – | 0.9992 |
| Kissinger equation | 156.34 | 5.61 | 0.9887 |
| Average | 156.12 | 5.61 | 0.9924 |

The $E$ and lg$A$ were calculated by the Friedman equation and Kissinger equation was shown in Table 1.

*Determination of the magnesite reaction mechanism function*

The integral form of Eq. 1 [17] can be written as:

$$F(a) = \int_0^{\alpha}\frac{d\alpha}{f(\alpha)} = \frac{A}{B}\int_{T_0}^{T} e^{-(E/RT)}dT \approx \frac{A}{B}\int_0^{T} e^{-(E/RT)}dT = \frac{AE}{\beta R}\int_{\infty}^{x}\frac{-e^{-x}}{x^2}dx = \frac{AE}{\beta R}\frac{e^{-x}}{x}\pi(x) \tag{4}$$

And the nature logarithm form of Eq. 4 can be expressed as:

$$\ln F(a) = \left[\ln\frac{AE}{R} + \ln\frac{e^{-x}}{x} + \ln\pi(x)\right] - \ln\beta \tag{5}$$

According to Eq. 5, a plot of $\ln F(a)$ versus $\ln\beta$ was constructed. Ten different values of $F(a)$ from document [18–22] were tested. The form of $F(a)$ that given the best straight line, which with high correlation coefficient ($r$-squared value) of linear regression analysis and the slope was equal to $-1.000$, was selected and the mechanism corresponding to this value of $F(a)$ was assigned as the mechanism for the reaction.

The conversions for $\beta = 15$, 20, 25, 35, and 40 K $min^{-1}$ were illustrated in Table 2. An appropriate temperature was randomly selected. Because when $\alpha < 0.10$ or $>0.90$, the reaction was in the initial stage or finished stage, they cannot represent the whole process of reaction truly, so the range of the conversions of this temperature should be within 0.10–0.90. We chose the corresponding conversions of $T = 931$ K for example.

The parameters calculated by this method were summarized in Table 3. From the results we can see that the slopes of D3, R2, and 3D were near to $-1.0000$ than others and with better correlation coefficient $r^2$, but which type of mechanism is the most probable one, needs further research.

When $0.10 < \alpha < 0.90$, several temperatures in Table 2 were chosen to calculate the slope $k$, correlation coefficient $r^2$, and intercept $B$ of D3, R2, and 3D mechanism function by the same method. The results were listed in Table 4,

**Table 2** Relation of temperature and conversion α at different heating rates $\beta$/K min$^{-1}$

| $T$/K | α | | | | |
|---|---|---|---|---|---|
| | $\beta = 15$ | $\beta = 20$ | $\beta = 25$ | $\beta = 35$ | $\beta = 40$ |
| 780 | 0.102 | 0.087 | 0.085 | 0.083 | 0.03 |
| 803 | 0.121 | 0.102 | 0.095 | 0.094 | 0.038 |
| 860 | 0.201 | 0.161 | 0.141 | 0.137 | 0.086 |
| 875 | 0.231 | 0.204 | 0.171 | 0.158 | 0.108 |
| 918 | 0.462 | 0.421 | 0.312 | 0.274 | 0.231 |
| 931 | 0.564 | 0.522 | 0.381 | 0.333 | 0.297 |
| 937 | 0.631 | 0.581 | 0.421 | 0.364 | 0.334 |
| 944 | 0.702 | 0.650 | 0.471 | 0.405 | 0.381 |
| 959 | 0.851 | 0.812 | 0.602 | 0.509 | 0.506 |
| 971 | 0.923 | 0.901 | 0.731 | 0.624 | 0.611 |
| 987 | 0.964 | 0.951 | 0.882 | 0.775 | 0.751 |

**Table 3** Basic data of $\lg F(\alpha)$ versus $\lg \beta$ curves of 10 types α of mechanism functions at $T = 931$ K ($\beta = 15, 20, 25, 35, 40$ K min$^{-1}$)

| Function | $B$ | $-k$ | $r^2$ |
|---|---|---|---|
| D4 | 0.27048 | 1.80364 | 0.99964 |
| R3 | 0.07422 | 2.68244 | 0.99249 |
| D3 | −0.50560 | 1.09984 | 0.99807 |
| R2 | −0.22249 | 1.04639 | 0.99886 |
| 3D | 0.20328 | 0.99211 | 0.99963 |
| A2 | 1.76512 | 1.62695 | 0.98449 |
| A1.5 | 3.25930 | 1.44995 | 0.92569 |
| A3/4 | 0.28039 | 0.52050 | 0.97898 |
| A1 | 0.24830 | 0.40784 | 0.96062 |
| A2/3 | −0.11188 | 0.52263 | 0.99886 |

**Table 4** Basic data of lg $F(\alpha)$ versus lg $\beta$ curves of three types α of mechanism functions ($\beta = 15$, 20, 25, 35, and 40 K min$^{-1}$).

| $T$/K | $B$ | $-k$ | $r^2$ |
|---|---|---|---|
| 875 | | | |
| D3 | −0.30592 | 0.99241 | 0.99901 |
| R2 | −0.94041 | 1.02789 | 0.99912 |
| 3D | −0.08275 | 1.01413 | 0.99959 |
| 918 | | | |
| D3 | −0.38578 | 0.98276 | 0.99123 |
| R2 | 0.02872 | 1.04425 | 0.98246 |
| 3D | −0.60103 | 1.0124 | 0.99949 |
| 937 | | | |
| D3 | 0.53808 | 0.98124 | 0.98976 |
| R2 | −0.07891 | 1.02314 | 0.99197 |
| 3D | −0.69100 | 1.0025 | 0.99956 |
| 944 | | | |
| D3 | 0.90124 | 0.90426 | 0.99912 |
| R2 | −0.72935 | 0.103413 | 0.99058 |
| 3D | −0.86041 | 0.99912 | 0.99924 |

they illustrated that the slope of 3D was the approach to −1.00000 and correlation coefficient $r^2$ was higher. So we can deduce that 3D mechanism function is the most probable one of magnesite thermal decomposition.

Meanwhile, the Malek method was also used to determine the most probable mechanism function. In the case of correlation coefficient close to one another, Malek method is the effective method, which is employed to further determine the most probable mechanism function [17]. The standard curve equation of mechanism function can be written as:

$$y(\alpha) = \frac{f(\alpha)F(\alpha)}{f(0.5)F(0.5)} \tag{6}$$

Experimental curve equation can be written as:

$$y(\alpha) = \left(\frac{T}{T_{0.5}}\right)^2 \frac{\left(\frac{d\alpha}{dt}\right)}{\left(\frac{d\alpha}{dt}\right)^{0.5}} \tag{7}$$

$F(\alpha)$ and $f(\alpha)$ are the reaction model, and $d\alpha/dt$ is obtained from TG curve. Plot $y(\alpha)$ versus α curves, if the experimental curve and the standard curve overlap or all experimental data points fall on a standard curve, the corresponding standard curve, $F(\alpha)$ or $f(\alpha)$, is the most probable mechanism function.

Take 20 K min$^{-1}$ as an example, the $y(\alpha)$ versus α curve is given in Fig. 3. Experimental curve is expressed by the dashed line and labeled by p.

From Fig. 4, it can be deduced that the magnesite decomposition is 3D mechanism. And the regression lines of anti-Jander kinetic model are illustrated in Fig. 5.

The average activation energy ($E$) calculated by anti-Jander equation mechanism was 168.77 kJ mol$^{-1}$, and more consistent with the activation energy (156.12 kJ mol$^{-1}$) was calculated through Friedman equation and Kissinger equation. However, the activation energy is related to the mechanism function; therefore, the activation energy calculated by

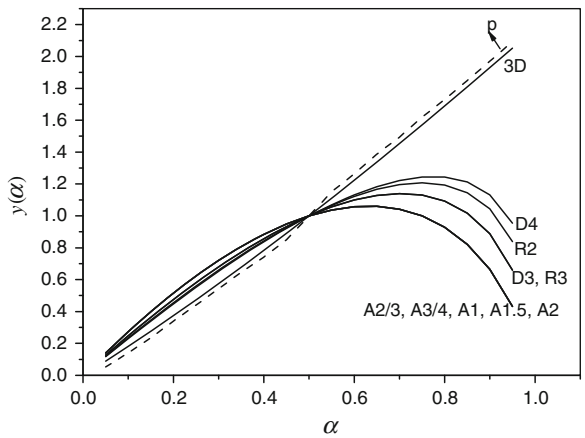


**Fig. 4** $y(\alpha) - \alpha$ curves of first phase

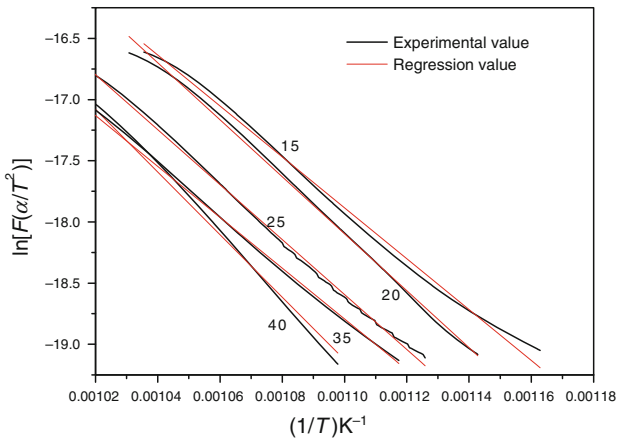


**Fig. 5** Linear regression of $\ln[F(\alpha)/T^2] - (1/T)$

anti-Jander equation mechanism has certain error with the activation energy calculated through Friedman equation and Kissinger equation.

Based on the above analysis, it is determined that the thermal decomposition of magnesite followed anti-Jander equation mechanism. Anti-Jander equation in integral form is given by:

$$F(\alpha) = [(1+\alpha)^{1/3} - 1]^2 \tag{8}$$

Differential form is given by:

$$f(\alpha) = 3(1+\alpha)^{2/3}[(1+\alpha)^{1/3} - 1]^{-1}/2 \tag{9}$$

The average of activation energy ($E$) calculated through Friedman equation and Kissinger equation was 156.12 kJ mol$^{-1}$, and the average of lg$A$-value was 5.61 s$^{-1}$. Therefore, the thermal decomposition of magnesite differential equation can be written as:

$$\frac{d\alpha}{dT} = \frac{10^{5.61}}{\beta}\exp\left(-\frac{18777.9}{T}\right)\left[\frac{3}{2}(1+\alpha)^{2/3}[(1+\alpha)^{1/3} - 1]^{-1}\right]$$

## Conclusions

a. A method Combined Friedman equation and Kissinger equation was applied to calculate the $E$ and lg$A$ values. A new multiple rate iso-temperature method and the Malek method were both used to determine the magnesite thermal decomposition mechanism function.
b. The process of thermal decomposition of magnesite was controlled by three-dimensional diffusion, and the kinetic function's differential form is $f(\alpha) = 3(1+\alpha)^{2/3}\ [(1+\alpha)^{1/3} - 1]^{-1}/2$.
c. The kinetic parameters of magnesite decomposition process obtained were: $E = 156.12$ kJ mol$^{-1}$, $A = 10^{5.61}$ s$^{-1}$, and the kinetic equation of the process was established.

**Acknowledgements** This study was supported by the Natural Science Foundation of China by a grant number 20876160 and National support project by a grant number 2006BAB02A11.

## References

1. Zhao YN, Zhu GZ. Thermal decomposition kinetics and mechanism of magnesium bicarbonate aqueous solution. Hydrometallurgy. 2007;89:217–23.
2. Özdemir M, Çakır D, Kıpçak İ. Magnesium recovery from magnesite tailings by acid leaching and production of magnesium chloride hexahydrate from leaching solution by evaporation. Int J Miner Process. 2009;1:209–12.
3. Demir F, Dönmez B. Optimization of the dissolution of magnesite in citric acid solutions. Int J Miner Process. 2008;1:60–4.
4. Wang HM. Status and development trend of China's magnesite. Cnin Non-Metal Min Indus Her. 2007;6:57–60.
5. Bertol CD, Cruz AP, Stulzer HK, Murakami FS, Silva MAS. Thermal decomposition kinetics and compatibility studies of primaquine under isothermal and non-isothermal conditions. J Therm Anal Calorim. 2010;102:187–92.
6. Liu P, Thomas PS, Ray AS, Guerbois JP. A TG analysis of the effect of calcination conditions on the properties of reactive magnesia. J Therm Anal Calorim. 2007;88:187–92.
7. L'vov BV. Mechanism and kinetics of thermal decomposition of carbonates. Thermochim Acta. 2002;386:1–16.
8. Lu RY, Dong J. Kinetics of thermal decomposition of magnesite in nitrogen. J Guizhou Univ Nat Sci. 2009;2:45–7.
9. Vyazovkin S, Sbirrazzuoli N. Isoconversional kinetic analysis of thermally stimulated processes in polymers. Macromol Rapid Commum. 2006;27:1515–32.
10. Peterson JD, Vyazovkin S, Wight CA. Kinetics of the thermal and thermooxidative degradation of polystyrene, polyethylene and polypropylene. Macromol Chem Phys. 2001;202:775–84.
11. Niu Sl, Han KH, Lu CM, Sun RY. Thermogravimetric analysis of the relationship among calcium magnesium acetate, calcium acetate and magnesium acetate. Appl Energy. 2010;87:2237–42.
12. Al-othman AA, Al-Farhan K, Mahfouz Refaat M. Kinetics analysis of nonisothermal decomposition of ($Mg_5(CO_3)_4(OH)_2 \cdot 4H_2O/5Cr_2O_3$) crystalline mixture. J King Saud Univ Sci. 2009;21:133–43.
13. Friedman HL. Kinetics of thermal degradation of char-forming plastics from thermogravimetry. Application to phenolic plastic. J Polym Sci C Polym Symp. 1964;6PC:285–92.
14. Li XY, Wu YQ, Gu DH, Gan FX. Thermal decomposition kinetics of nickel(II) and cobalt(II) azo barbituric acid complexes. Thermochim Acta. 2009;493:85–9.
15. Zheng HX, Liao XS, Wang Q, J Li. TG kinetics of decomposition of magnesite power and its pellet. J Univ Sci Technol Liaoning. 2008;31:29–31.
16. Kisssinger HE. Reaction kinetics in different thermal analysis. Anal Chem. 1957;29:1702.
17. Hu RZ, Shi QZ. Thermal analysis kinetics. Beijing: Science Press; 2001.
18. Samtain M, Dollimore D, Alexander KS. Comparison of dolomite decomposition kinetics with related carbonates and the effect of procedural variables on its kinetics parameters. Thermochim Acta. 2002;392–393:135–45.
19. Ning ZQ, Zhai YC, Sun LQ. Study on the thermal decomposition kinetics of magnesium hydroxide. J Mol Sci. 2009;25:27–30.

20. Zheng Y, Chen XH, Zhou YB, Zheng C. The decomposition mechanism of $CaCO_3$ and its kinetics parameters. J Huazhong Univ Sci Technol. 2002;12:86–8.
21. Zhang BS, Liu JZ, Zhou JH, Feng ZG, Qin KF. Experimental study on the impaction of particle size to limestone decomposition kinetics by thermogravimetry. Proc CSEE. 2010;30:51–5.
22. Wang SJ, Lu JD, Zhou H, Hu ZJ, Zhang BT. Kinetics model study on thermal decomposition of limestone particles. J Eng Thermophys. 2003;24:699–702.